Original Article

J Korean Soc Radiol 2019;80(1):105-116
https://doi.org/10.3348/jksr.2019.80.1.105
pISSN 1738-2637 / eISSN 2288-2928

대한영상의학회지

Dual-Layer Spectral Detector CT Discography of the Lumbar Spine: A Preliminary Study

이층 스펙트럴 CT를 이용한 요추 추간판 조영술의 유용성에 대한 예비 연구

Hee-Dong Chae, MD[1], Sung Hwan Hong, MD[1]*, Ja-Young Choi, MD[1], Hye Jin Yoo, MD[1], Sun Jeong Moon, MD[1], Min-Yung Chang, MD[2]

[1]Department of Radiology, Seoul National University Hospital, Seoul, Korea
[2]Department of Radiology, National Health Insurance Service Ilsan Hospital, Goyang, Korea

Received November 13, 2018
Revised November 14, 2018
Accepted November 21, 2018

***Corresponding author**
Sung Hwan Hong, MD
Department of Radiology,
Seoul National University
College of Medicine,
103 Daehak-ro, Jongno-gu,
Seoul 03080, Korea.

Tel 82-2-2072-3217
Fax 82-2-743-7418
E-mail drhong@snu.ac.kr

ORCID iDs
Sung Hwan Hong
https://orcid.org/0000-0003-2302-1341
Hee-Dong Chae
https://orcid.org/0000-0003-2624-1606

Purpose To assess the feasibility of spectral detector CT (SDCT) with axial maximum-intensity projection (MIP) reconstruction for the evaluation of lumbar CT discography.

Materials and Methods We retrospectively evaluated 44 disc levels from 18 patients who underwent CT discography on a dual-layer SDCT between May 2016 and July 2017. We compared the distribution of contrast material between conventional CT and SDCT-based iodine maps using the Jaccard index (JI) and Dice similarity coefficient (DSC). Qualitative analysis of the post-discogram features was done according to the Dallas discogram description, and changes in reading time and diagnostic confidence were analyzed.

Results The intermethod variability between conventional CT and SDCT was good, with a mean DSC of 0.93 and a mean JI of 0.87. The mean sensitivity and positive predictive value of the SDCT-based method were 90% and 96%, respectively. The addition of SDCT-based axial MIP iodine maps increased the diagnostic confidence ($p = 0.025$) and reduced the reading time in both reviewers ($p < 0.001$).

Conclusion SDCT discography demonstrates the distribution of contrast medium within the disc similarly to conventional CT. Additionally, axial MIP iodine maps using SDCT allow for the fast evaluation of disc pathology with reduced reading time and can increase diagnostic confidence.

Index terms Tomography, X-Ray Computed; Intervertebral Disc Degeneration; Contrast Media

INTRODUCTION

Lumbar discography is a useful procedure in the evaluation and potential treatment

planning of presumed discogenic pain. Discography is also used to diagnose lateral disc herniation, choose fusion levels on preoperative planning, identify symptomatic discs among multiple degenerative discs, and as a therapeutic intervention when steroid is injected intradiscally (1, 2). CT discography has essentially become the standard in performing discography because a more comprehensive view of disc pathology is provided with the addition of detailed cross-sectional imaging. However, accurate evaluation of CT discography is sometimes difficult because the attenuation of iodinated contrast material on CT is similar to that of an adjacent vertebral body endplate or an osteophyte (3).

Dual-energy CT can resolve this problem because of its material separation capability. Because attenuation of materials and tissues differs at different photon energies, dual-energy CT allows for quantification of materials and tissues (4, 5). Utilizing this ability, spectral CT has been successfully applied to musculoskeletal imaging to confirm the presence of monosodium urate crystals in and around joints in gout arthropathy (6), identify bone marrow edema (7), and visualize tendons and ligaments (8).

However, relatively few technical changes in the procedure have occurred since the advent of discography, and the application of spectral CT to discography is very limited. Therefore, this study aimed to assess the feasibility of dual-layer spectral detector CT (SDCT) with axial maximum-intensity projection (MIP) reconstruction for the evaluation of lumbar CT discography.

MATERIALS AND METHODS

Our Institutional Review Board approved this retrospective study with a waiver of informed consent.

STUDY POPULATION

Between May 2016 and July 2017, 30 patients who were suspected to suffer from chronic discogenic pain underwent CT discography at our institution. Of these patients, 18 (mean age

Table 1. Characteristics of the Study Population

Characteristics	Value
Number of patients	18
Sex	
Male	6
Female	12
Age (year)*	54.7 ± 8.6 (40–73)
Male	52.2 ± 10.9 (40–67)
Female	56.0 ± 7.5 (44–73)
Disc level (*n* = 44)	
L2–3	7
L3–4	10
L4–5	13
L5–S1	14

*Data are presented as the mean ± standard deviation, with the range in parentheses.

54.7 ± 8.6 years; range 40–73 years) who had CT examinations on a dual-layer SDCT constituted our study population. Our study comprised 6 men (mean age 52.2 ± 10.9 years; range 40–67 years) and 12 women (mean age 56.0 ± 7.5 years; range 44–73 years). Discography was performed at 44 disc levels in these 18 patients (7 at L2–3; 10 at L3–4; 13 at L4–5; 14 at L5–S1) (Table 1).

LUMBAR DISCOGRAPHY AND POST-DISCOGRAM CT ACQUISITION

Discography was performed using a routine posterolateral, extrapedicular approach. A single-needle technique using a 22-gauge spinal needle accessed the center of each disc space. Nonionic contrast medium (Iopamiro 300; Bracco, Milan, Italy) was injected manually under fluoroscopic guidance.

All CT examinations were performed with a dual-layer SDCT system (IQon Spectral CT, Philips Healthcare, Best, The Netherlands). All the patients were scanned using a 120 kVp tube voltage, with automatic tube current modulation and mAs adapted to the patient body size. The detector configuration was 64 × 0.625 mm. The pitch ranged from 0.52 to 0.55, and a gantry rotation time of 0.4 seconds was used. On the SDCT, conventional CT images and spectral based images (SBIs) are reconstructed from the same scan in two ways. In one reconstruction pathway, data from each detector layer are combined to generate conventional CT images. The second reconstruction combines data from both detector layers to create projection-based SBIs, which then are used to generate spectral results, including iodine density maps. In this study, conventional CT images were reconstructed using iDose4 (Philips Healthcare) level 2 with a slice thickness of 1 mm and increment of 1 mm using the bone/soft tissue algorithm. Sagittal and coronal reformatted images with a slice thickness and increment of 2 mm were obtained using the soft tissue algorithm. Additionally, SBIs were reconstructed at a slice thickness and increment of 1 mm using a dedicated spectral image reconstruction algorithm with a spectral level of 2.

QUANTITATIVE IMAGE ANALYSIS

To quantify the accuracy of iodine-bone separation on SDCT, we compared the distribution of contrast material within the disc between conventional CT images and SDCT-based iodine maps. Regions of interest (ROIs) based on the manual segmentations on conventional CT images served as reference standards for comparison. The detailed protocol for image reconstruction was as follows.

IODINE-BONE SEPARATION ON CONVENTIONAL CT IMAGES

One reader (HDC) manually segmented intervertebral discs on the sagittal plane for each slice using a dedicated workstation (IntelliSpace Portal Version 7.0, Philips Healthcare). An outline was drawn around the boundary of each intervertebral disc to include all the areas with contrast media. Care was taken to prevent the inclusion of the subchondral bone plate. MIP images were created in the axial plane, and ROIs were chosen by adjusting the window width and level to delineate the area with contrast material.

IODINE-BONE SEPARATION ON SDCT IMAGES

One radiologist (HDC) and one radiologic technologist with 3 years of experience in radiology research created SDCT-based ROIs of contrast material. Iodine density maps were reconstructed automatically from SBIs, and we used the density maps to create axial MIP images for each disc using the vendor-provided spectral viewer (Spectral Diagnostics Suite, Philips Healthcare). Slab thickness was properly chosen to include all disc regions with contrast media. ROIs were determined by adjusting the threshold so that most of the area with contrast material could be included (Fig. 1).

COMPARISON OF THE CONVENTIONAL AND SDCT-BASED SEPARATION

The accuracy of SDCT-based iodine-bone separation was evaluated against conventional CT using the Dice similarity coefficient (DSC) and the Jaccard index (JI, also known as intersection over union) (9, 10). They are commonly used measures for quantifying the degree of overlap between two segmentations and are defined as follows:

$$DSC(A, B) = \frac{2 \times |A \cap B|}{|A| + |B|}$$

and

$$JI(A, B) = \frac{|A \cap B|}{|A \cup B|} = \frac{|A \cap B|}{|A| + |B| - |A \cap B|}$$

where A and B represent areas of two different segmentations. A value of 1 denotes perfect similarity (identity) between two segmentations, while a value of 0 indicates no overlap. The sensitivity (recall) and positive predictive value (PPV) were also reported. To calculate these metrics, the ROI of each disc from MIP images of SDCT was superimposed on the manually segmented ROI from conventional CT images. Rigid-body registration of two ROI masks were performed using TurboReg (11), an ImageJ (ver 1.51; National Institutes of Health, Bethesda, MD, USA) plug-in for automatic image registration. Overlap measures were then

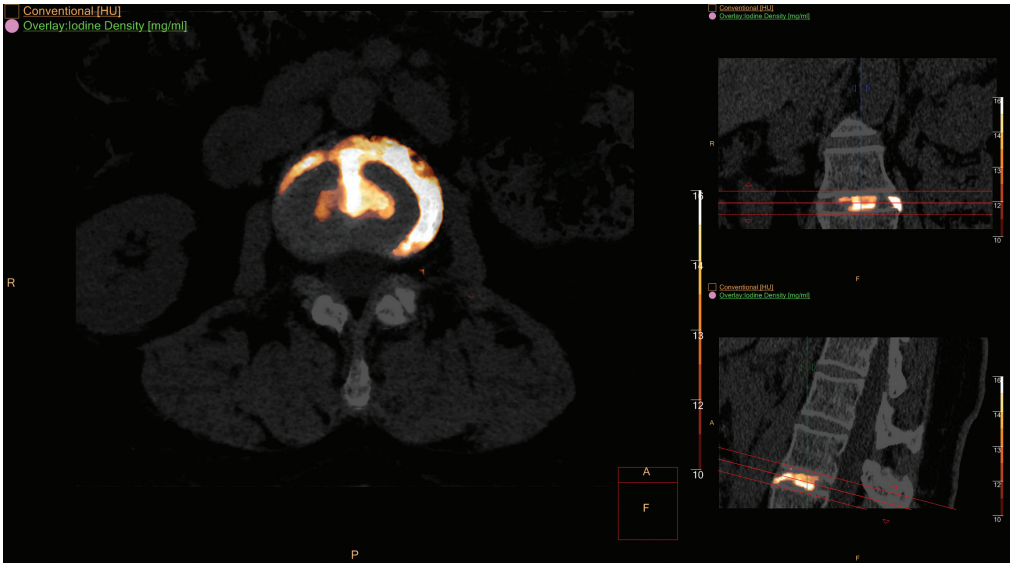

Fig. 1. Screenshot showing a vendor-provided spectral viewer. The slab thickness was properly chosen to include all disc regions with contrast media on the sagittal plane. Subsequently, color-coded axial maximum-intensity projection images were created using the spectral-based iodine density maps.

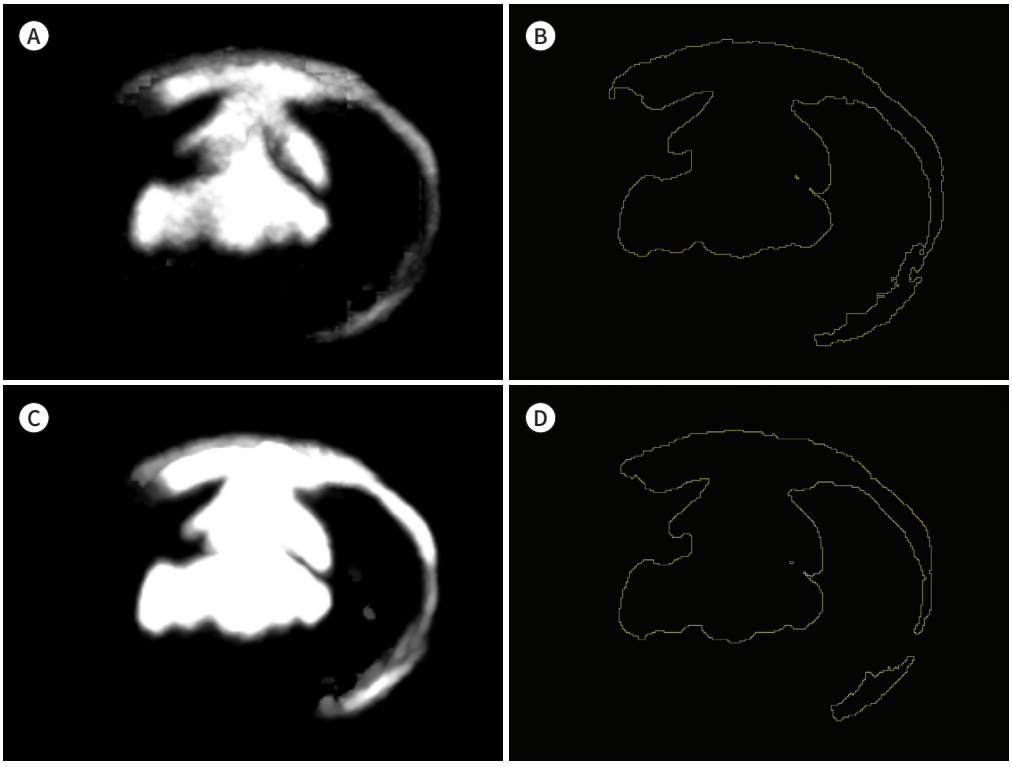

Fig. 2. Axial MIP iodine map images obtained from conventional CT and SDCT discography.
A, B. An axial MIP image and corresponding ROI obtained from conventional CT discography. The ROI was selected to include the area with contrast material by properly adjusting the window width and level.
C, D. An axial MIP image and ROI of the same disc level obtained from SDCT are similar to those obtained from conventional CT discography. The Jaccard index between the two ROIs is 0.91 and the Dice similarity coefficient is 0.95.
MIP = maximum-intensity projection, ROI = region of interest, SDCT = spectral detector CT

calculated using another ImageJ plug-in, DetectionEvaluationJ (12) (Fig. 2).

QUALITATIVE IMAGE ANALYSIS

Qualitative analysis of the post-discogram features were done by two board-certified musculoskeletal radiologists (HDC and HSH, with 3 and 20 years of experience in musculoskeletal radiology, respectively). Data sets were reviewed in a commercial picture archive and communication systems (PACS) program (INFINITT PACS, INFINITT Healthcare, Seoul, Korea). With regard to CT discography features, degeneration and annular disruption were graded according to the original Dallas discogram description (13). Degeneration is based on the percentage area of contrast material within the degenerated annulus fibrosus on the axial image and was rated as follows: grade 0, normal; grade 1, local degeneration (< 10%); grade 2, partial degeneration (< 50%); and grade 3, total degeneration (> 50%). Annular disruption was evaluated according to the radial extent of contrast material moving away from the nucleus pulposus and was graded as follows: grade 0, contrast material within a nucleus pulposus; grade 1, contrast material extending radially into the inner annulus; grade 2, contrast material extending into the outer annulus; and grade 3, contrast material extending beyond the outer annulus.

Two separate reading sessions were conducted to investigate the added value of axial MIP iodine maps to the reliability and efficiency of CT discography evaluation. Both reviewers assessed CT discography features using the Dallas discogram description and recorded diagnostic confidence and reading time during each session. Diagnostic confidence was scored with a four-point scale: grade 1, very unsure; grade 2, less confident; grade 3, moderately confident; grade 4, highly confident. For the evaluation of time efficiency, the time from the

start of the reading until the final diagnosis of CT discography features was recorded by both reviewers for each disc level. The time for loading the images into the PACS viewer was not included in the measurements. A training session was implemented before the first session was begun using separate data sets. At the first reading session, the reviewers were only provided with conventional CT data sets, which comprised axial images obtained parallel to the disc plane and sagittal and coronal reformatted images. The reviewers were allowed to adjust magnification and window settings as necessary. After four weeks, the same assessment was repeated with the addition of axial MIP iodine maps reconstructed from SBIs to the same conventional CT data sets.

STATISTICAL ANALYSIS

The mean values and 95% confidence intervals (CIs) of DSC, JI, sensitivity, and PPV were calculated to evaluate the accuracy of SDCT-based iodine separation. Interobserver variability of the SDCT-based iodine-bone separation method was also assessed by calculating DSC and JI between two different ROIs created by two researchers. A DSC value equal to or higher than 0.7 was considered a good agreement between 2 compared measurements (14).

Interobserver variability between two readers in the qualitative evaluation of CT discography features was assessed using weighted κ statistics with linear weighting. Kappa values <0.40 signified poor agreement, 0.41–0.60 moderate agreement, 0.61–0.80 good agreement, and ≥0.81 excellent agreement. Ninety-five-percent CIs were calculated to compare kappa values using the method suggested by Fleiss et al. (15). Differences in diagnostic confidence and reading time between two reading sessions were analyzed by using the Wilcoxon signed rank test and the paired *t* test, respectively. Statistical analyses were performed using SPSS for Windows (ver. 22.0; IBM Corp., Armonk, NY, USA) and MedCalc (ver. 12.2.1; MedCalc Software, Mariakerke, Belgium). A *p* value of < 0.05 was considered to indicate a significant difference.

RESULTS

QUANTITATIVE IMAGE ANALYSIS

The interobserver variability for the SDCT-based method showed good agreement between two reconstructions, with mean DSC and JI values of 0.91 (95% CI, 0.88–0.93) and 0.84 (95%

Table 2. Interobserver Variability of SDCT-Based Iodine-Bone Separation and Intermethod Variability Between Conventional CT and SDCT-Based Methods

	DSC	JI	Sensitivity (%)	PPV (%)
Interobserver variability				
Mean	0.91 (0.88–0.93)	0.84 (0.80–0.88)	-	-
Range	0.43–0.98	0.27–0.96	-	-
Intermethod variability				
Mean	0.93 (0.92–0.94)	0.87 (0.85–0.89)	90 (88–93)	96 (95–97)
Range	0.76–0.98	0.61–0.97	64–99	86–99

Data in parentheses are 95% confidence intervals.
DSC = Dice similarity coefficient, JI = Jaccard index, PPV = positive predictive value, SDCT = spectral detector CT

CI, 0.80–0.88), respectively. The intermethod variability was good between conventional CT and SDCT-based methods. The mean DSC between the two methods was 0.93 (95% CI, 0.92–0.94), and the mean JI was 0.87 (95% CI, 0.85–0.89). The mean sensitivity and PPV of SDCT-based method were 90% (95% CI, 88–93%) and 96% (95% CI, 95–97%), respectively (Table 2).

QUALITATIVE IMAGE ANALYSIS

Good interobserver agreement was observed in the evaluation of CT discography features between two reviewers. Using conventional CT images only, weighted kappa values were 0.76 (95% CI, 0.60–0.93) for degeneration and 0.64 (95% CI, 0.38–0.90) for annular disruption. When axial MIP iodine maps were added to conventional CT data sets, there was no significant change in the degree of agreement, with weighted kappa values of 0.72 (95% CI, 0.55–0.89) for degeneration and 0.68 (95% CI, 0.45–0.92) for annular disruption ($p > 0.05$, respec-

Table 3. Qualitative Analysis of Conventional and Spectral Detector Computed Tomography Discography

Parameter	Session 1		Session 2	
	Reviewer 1	Reviewer 2	Reviewer 1	Reviewer 2
Degeneration				
Grade 0	1	2	1	2
Grade 1	4	6	4	7
Grade 2	10	7	10	9
Grade 3	29	29	29	26
Interobserver variability*	0.76 (0.60–0.93)		0.72 (0.55–0.89)	
Annular disruption				
Grade 0	1	2	1	2
Grade 1	2	1	2	1
Grade 2	4	7	2	8
Grade 3	37	34	39	33
Interobserver variability*	0.64 (0.38–0.90)		0.68 (0.45–0.92)	
Diagnostic confidence[†] [‡]				
Grade 1	0 (0)	0 (0)	0 (0)	0 (0)
Grade 2	0 (0)	0 (0)	0 (0)	0 (0)
Grade 3	19 (43)	16 (36)	9 (20)	6 (14)
Grade 4	25 (57)	28 (64)	35 (80)	38 (86)
Reading time (s)[§] [‖]	33.3 ± 23.8	27.9 ± 12.8	18.1 ± 8.8	12.3 ± 4.4

Degeneration grade: 0 = normal, 1 = local degeneration (< 10%), 2 = partial degeneration (< 50%), 3 = total degeneration (> 50%). Annular disruption grade: 0 = contrast material within the nucleus pulposus, 1 = contrast material extending radially into the inner annulus, 2 = contrast material extending into the outer annulus, 3 = contrast material extending beyond the outer annulus. Diagnostic confidence score: 1 = very unsure, 2 = less confident, 3 = moderately confident, 4 = highly confident.

*Linear weighting was used for kappa values. Data in parenthesis are 95% confidence intervals.

[†]Data in parenthesis are percentages.

[‡]$p = 0.025$ for both reviewer 1 and reviewer 2 between two sessions. *p* values were determined by the Wilcoxon signed rank test.

[§]Data are mean ± standard deviation.

[‖]$p < 0.001$ for reviewer 1 and reviewer 2 between two sessions. *p* values were determined using the paired *t* test.

s = second

tively).

The addition of axial MIP iodine maps significantly increased diagnostic confidence in both reviewers (p = 0.025). The number of disc levels evaluated with high diagnostic confidence increased from 25 (57%) to 28 (64%) in reviewer 1 and from 35 (80%) to 38 (86%) in reviewer 2. Reading time was significantly decreased from 33.3 seconds ± 23.8 to 18.1 seconds

Fig. 3. CT discography images of the L4-5 disc in a 44-year-old female patient.
A. An axial CT discography image showing annular disruption at the 6 o'clock position (arrow). This disc was evaluated to have localized annular degeneration (grade 1) and annular disruption extending to the outer annulus (grade 2).
B. Corresponding spectral CT-based axial maximum-intensity projection iodine map also demonstrates a fairly similar shape of the annular disruption (arrow). There are several artifacts due to incomplete iodine-bone separation around the posterior element of the spine (arrowhead).

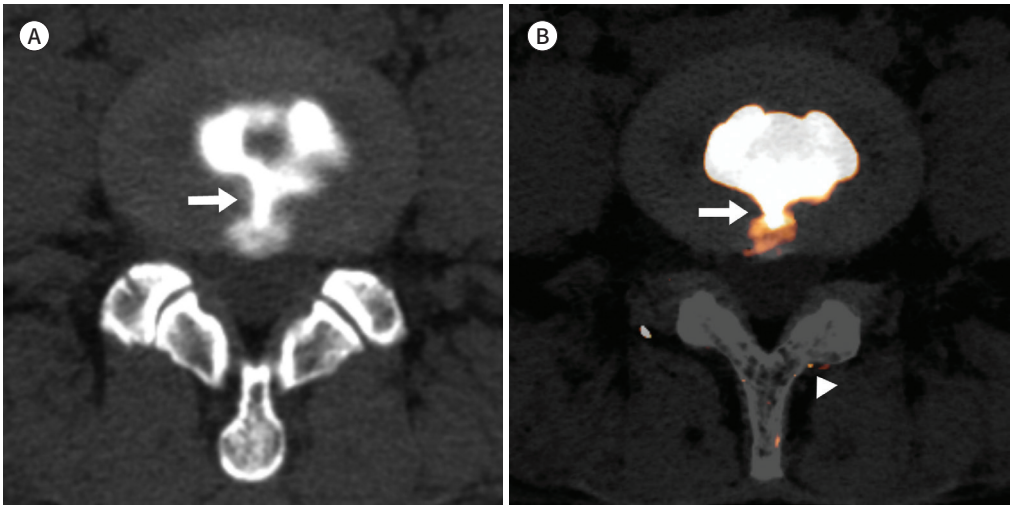

Fig. 4. CT discography images of the L5-S1 disc in a 54-year-old female patient.
A. An axial conventional CT image showing a curvilinear, highly attenuated lesion (arrow) suspected to be a concentric annular disruption on the left posterolateral side of the L3-4 disc.
B. In the corresponding spectral CT-based axial maximum-intensity projection iodine map, there is no iodine in the curvilinear area seen on conventional CT. The lesion was confirmed to be a ring apophysis and the disc was evaluated to have annular disruption extending to the inner annulus (grade 1).

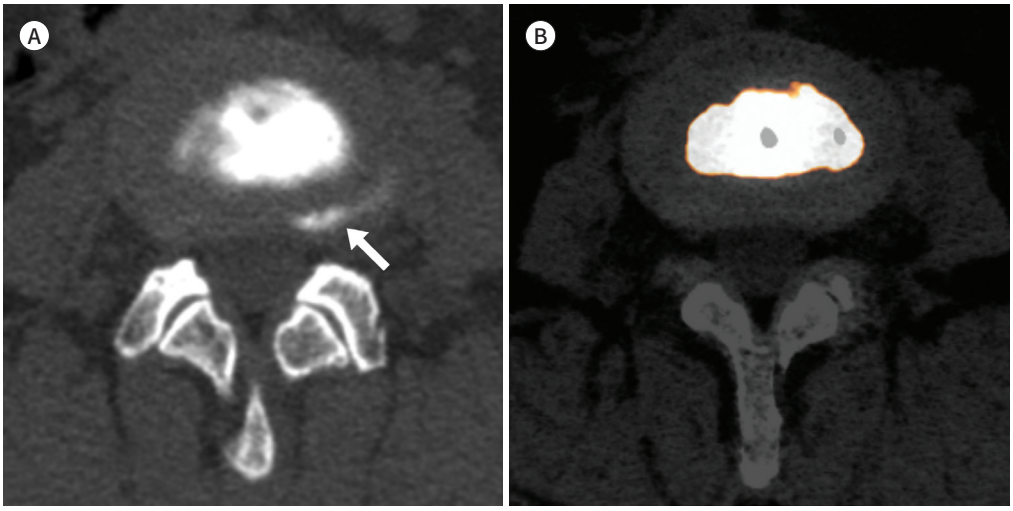

± 8.8 for reviewer 1 ($p < 0.001$) and from 27.9 seconds ± 12.8 to 12.3 seconds ± 4.4 for reviewer 2 ($p < 0.001$) between two interpretation session (Table 3). Representative cases are shown in Figs. 3, 4.

DISCUSSION

In our study, the distribution of contrast material within intervertebral discs obtained by SDCT-based iodine-bone separation was well correlated with that of conventional CT. Interobserver variability analysis revealed good agreement between two SDCT-based axial MIP iodine maps reconstructed by two independent researchers, showing that this approach is a highly reproducible method. On qualitative analysis, the addition of SDCT-based axial MIP images increased diagnostic confidence and reduced reading time in both reviewers.

Although there are some controversies regarding the clinical validity of discography (16, 17), many investigators have shown that there is evidence supporting the diagnostic benefit of discography, in particular following the advent of CT discography (1, 2, 18, 19). For the description of CT discographic findings, the Dallas discogram description system is usually used (13, 20), and the axial-plane images are important to evaluate the exact extent of radial tear and annular degeneration. However, the similar attenuation of contrast media and bony endplates makes it difficult to determine the exact distribution of contrast material. SDCT, which has recently been increasingly used in clinical practice and research, can provide a solution to this problem.

In conventional CT, materials with different chemical compositions can show similar Hounsfield numbers, causing difficulty in differentiating different types of tissues. Although the atomic numbers of calcium and iodine are considerably different, bone and contrast media can be represented by the same attenuation coefficient, depending on the concentration of each material. In dual-energy CT, however, the simultaneous measurement at different X-ray energies allows the characterization of any material by its effective atomic number and effective mass density. Through a mathematical transformation of basis, material-specific images can be generated, allowing the differentiation of different materials (e.g., bone and contrast media) (21, 22).

A search of the medical literature revealed only one investigation of CT discography using dual-energy CT (23). Jun (23) evaluated the feasibility of automatic bone removal on dual-energy CT discography using the porcine cadaver spine. They compared the area of intradiscal contrast collection between dual-energy and conventional CT images. In accordance with our study, they have shown that there was a strong correlation (correlation coefficient, 0.991; $p < 0.001$) in the area with contrast media between bone-removal images made from dual-energy CT discography and subtraction images. However, their method comparing the total area of contrast material cannot reflect the complex distribution pattern of degenerated discs.

In this study, the addition of axial MIP iodine maps to conventional CT images led to an increase in diagnostic confidence and a marked reduction in reading time. Because a single axial slice reflects only the disc portion within the slice thickness, the distribution of contrast material within the entire disc can be evaluated only by viewing a series of sequential axial

images. Coronal and sagittal images should also be referenced if the disc is accompanied by a complex degenerative change. The axial MIP iodine maps reconstructed from SDCT discography are analogous to the diagram of the Dallas discogram description, reflecting the whole intervertebral disc, and hence can be used to overview the disc pathology.

This investigation had several limitations. First, our sample size was relatively small. Further studies with larger samples are necessary. Second, the imaging modality could not be blinded to the reviewers, which could serve as a potential source of bias. Third, due to various artifacts in SDCT (24), the iodine density maps may also contain pixels with calcium, and the accuracy of iodine quantification may be reduced in areas with low iodine concentrations. Finally, because of the lack of a reference standard, it is difficult to determine the diagnostic performance of reviewers. Although we used manually segmented ROIs as a reference standard for the regions with contrast material, the segmentation was not verified with histopathologic examination. Since it is not possible to assess histologically the distribution of contrast medium in the disc, we assumed that manual segmentation by a radiologist would best reflect the daily practice of CT discography interpretation.

In conclusion, SDCT discography can demonstrate the distribution of contrast medium within the intervertebral disc similarly to conventional CT. Additionally, the axial MIP iodine map images using SDCT-based iodine-bone separation may serve as a useful tool for a fast evaluation and provide a good overview of disc pathology, enhancing diagnostic confidence.

Conflicts of Interest

The authors have no potential conflicts of interest to disclose.

REFERENCES

1. Saboeiro GR. Lumbar discography. *Radiol Clin North Am* 2009;47:421-433
2. Manchikanti L, Benyamin RM, Singh V, Falco FJ, Hameed H, Derby R, et al. An update of the systematic appraisal of the accuracy and utility of lumbar discography in chronic low back pain. *Pain Physician* 2013;16:SE55-SE95
3. Myung JS, Lee JW, Park GW, Yeom JS, Choi JY, Hong SH, et al. MR diskography and CT diskography with gadodiamide-iodinated contrast mixture for the diagnosis of foraminal impingement. *AJR Am J Roentgenol* 2008;191:710-715
4. Kaza RK, Ananthakrishnan L, Kambadakone A, Platt JF. Update of dual-energy CT applications in the genitourinary tract. *AJR Am J Roentgenol* 2017;208:1185-1192
5. Johnson TR. Dual-energy CT: general principles. *AJR Am J Roentgenol* 2012;199:S3-S8
6. Bongartz T, Glazebrook KN, Kavros SJ, Murthy NS, Merry SP, Franz WB 3rd, et al. Dual-energy CT for the diagnosis of gout: an accuracy and diagnostic yield study. *Ann Rheum Dis* 2015;74:1072-1077
7. Kaup M, Wichmann JL, Scholtz JE, Beeres M, Kromen W, Albrecht MH, et al. Dual-energy CT-based display of bone marrow edema in osteoporotic vertebral compression fractures: impact on diagnostic accuracy of radiologists with varying levels of experience in correlation to MR imaging. *Radiology* 2016;280:510-519
8. Glazebrook KN, Brewerton LJ, Leng S, Carter RE, Rhee PC, Murthy NS, et al. Case-control study to estimate the performance of dual-energy computed tomography for anterior cruciate ligament tears in patients with history of knee trauma. *Skeletal Radiol* 2014;43:297-305
9. Dice LR. Measures of the amount of ecologic association between species. *Ecology* 1945;26:297-302
10. Bakic PR, Carton AK, Kontos D, Zhang C, Troxel AB, Maidment AD. Breast percent density: estimation on digital mammograms and central tomosynthesis projections. *Radiology* 2009;252:40-49
11. Thévenaz P, Ruttimann UE, Unser M. A pyramid approach to subpixel registration based on intensity. *IEEE*

Trans Image Process 1998;7:27-41

12. Heras J. DetectionEvaluationJ Available at. https://joheras.github.io/DetectionEvaluationJ. Accessed Jun 27, 2018
13. Sachs BL, Vanharanta H, Spivey MA, Guyer RD, Videman T, Rashbaum RF, et al. Dallas discogram description. A new classification of CT/discography in low-back disorders. *Spine (Phila Pa 1976)* 1987;12:287-294
14. Bagci AM, Lee SH, Nagornaya N, Green BA, Alperin N. Automated posterior cranial fossa volumetry by MRI: applications to Chiari malformation type I. *AJNR Am J Neuroradiol* 2013;34:1758-1763
15. Fleiss JL, Levin B, Cho Paik M. *Statistical methods for rates and proportions*. 3rd ed. New York, NY: John Wiley & Sons, 2013
16. Chou R, Loeser JD, Owens DK, Rosenquist RW, Atlas SJ, Baisden J, et al. Interventional therapies, surgery, and interdisciplinary rehabilitation for low back pain: an evidence-based clinical practice guideline from the American Pain Society. *Spine (Phila Pa 1976)* 2009;34:1066-1077
17. Cuellar JM, Stauff MP, Herzog RJ, Carrino JA, Baker GA, Carragee EJ. Does provocative discography cause clinically important injury to the lumbar intervertebral disc? A 10-year matched cohort study. *Spine J* 2016;16:273-280
18. Bernard TN Jr. Lumbar discography followed by computed tomography. Refining the diagnosis of low-back pain. *Spine (Phila Pa 1976)* 1990;15:690-707
19. Manchikanti L, Glaser SE, Wolfer L, Derby R, Cohen SP. Systematic review of lumbar discography as a diagnostic test for chronic low back pain. *Pain Physician* 2009;12:541-559
20. Schellhas KP, Pollei SR, Gundry CR, Heithoff KB. Lumbar disc high-intensity zone. Correlation of magnetic resonance imaging and discography. *Spine (Phila Pa 1976)* 1996;21:79-86
21. Johnson T, Fink C, Schönberg SO, Reiser MF. *Dual energy CT in clinical practice.* Berlin: Springer, 2011
22. Patino M, Prochowski A, Agrawal MD, Simeone FJ, Gupta R, Hahn PF, et al. Material separation using dual-energy CT: current and emerging applications. *Radiographics* 2016;36:1087-1105
23. Jun WS. Dual-energy CT discography: experimental study for validation of automated bone removal application [dissertation]. Seoul: Seoul National University, 2009
24. Mallinson PI, Coupal T, Reisinger C, Chou H, Munk PL, Nicolaou S, et al. Artifacts in dual-energy CT gout protocol: a review of 50 suspected cases with an artifact identification guide. *AJR Am J Roentgenol* 2014;203:W103-W109

대한영상의학회지

이층 스펙트럴 CT를 이용한 요추 추간판 조영술의 유용성에 대한 예비 연구

채희동[1] · 홍성환[1]* · 최자영[1] · 류혜진[1] · 문선정[1] · 장민영[2]

목적 본 연구에서는 이층 스펙트럴 전산화단층촬영(이하 CT) 및 최대강도투사(maximum-intensity projection; 이하 MIP)를 사용한 요추 추간판 조영술의 유용성을 평가하였다.

대상과 방법 2016년 5월부터 2017년 7월 사이에 스펙트럴 CT를 이용하여 요추 CT 추간판 조영술을 시행한 18명의 환자 44개의 추간판을 후향적으로 분석하였다. Jaccard 지표(Jaccard index; 이하 JI) 및 Dice 유사도 계수(Dice similarity coefficient; 이하 DSC)를 이용하여 고식적 CT와 스펙트럴 CT에서의 요오드 분포를 비교하였다. 정성적 평가는 디스크 조영술 소견을 Dallas 추간판 조영술 기술 기준(Dallas discography description)을 사용하여 분석하였고, 스펙트럴 CT MIP 영상을 추가하였을 때 판독 시간 및 판독 확신도를 분석하였다.

결과 두 방법 간의 일치도는 DSC 0.93, JI 0.87로 우수한 일치도를 보였다. 고식적 CT에서의 요오드 분포를 기준으로 하였을 때 스펙트럴 CT의 민감도 및 양성 예측도는 90% 및 96%의 진단능을 보였다. 스펙트럴 CT 기반의 MIP 영상을 추가하였을 때 두 명의 평가자 모두 판독 시간의 감소 ($p < 0.001$) 및 판독 확신도의 향상($p = 0.025$) 결과를 보였다.

결론 스펙트럴 CT 디스크 조영술은 고식적 CT와 거의 유사한 조영제 분포를 보이며 스펙트럴 CT 기반 MIP 영상을 추가하였을 때 유의한 판독 시간 단축 및 판독 확신도 향상의 결과를 보인다.

[1]서울대학교병원 영상의학과, [2]국민건강보험 일산병원 영상의학과